

Fusion of wearable sensors and mobile haptic robot for the assessment in upper limb rehabilitation

Lucia Saracino¹, Emanuele Ruffaldi¹, Alessandro Graziano¹ and Carlo Alberto Avizzano¹

Abstract—Robot based rehabilitation is gaining traction also thanks to a generation of light and portable devices. This type of rehabilitation offers a high degree of flexibility in the design of interaction software and therapeutic process. There is therefore the need to perform assessment of the patient upper limb state during and after treatment. This paper presents the integration and fusion of a portable rehabilitation robot called MOTORE++ with a wearable tracking system for assessment purposes. The wearable system is based on inertial units together with EMG signals. The combination of the data from both the devices allows to partially evaluate the physiological condition of the user and the influence of the robot in the rehabilitation procedure. Results of an experimental campaign with patients is presented. This work opens also a spectrum of possible developments of adaptive behavior of the robot in the interaction with the patient.

I. INTRODUCTION

In the last years, robot-assistive systems are gradually taking hold in the medical rehabilitation scenarios. This brought the necessity to define criteria able to evaluate the quality of the devices (and the related exercises) in the rehabilitation procedure. Indeed, the development of wearable biometric capture systems, and new sensor-fusion based techniques, improve the knowledge about subject performance during the exercises and his pathological state. Recently, biomedical researches in the contest of post-stroke upper limb rehabilitation [22] have invoked new contributions from robotics technology, whose applications have to be versatile enough to analyze and treat neurological and post-traumatic disorders [11][13]. As underlined in [14], kinematic measurements (such as force/torque trends) [4] [18] [23] and electromyography [2], together with reliable motion reconstruction [12], could provide further insights on the description of bodily function and a further analysis of cinematic coordination between humans and robots [21].

This work addresses upper-limb rehabilitation after-stroke, performed with a 2D planar device called MOTORE++[20], [1]. To obtain a set of parameters that evaluates and adapts the robot behavior for each patient condition, we have developed and presented a method that assembles and processes data from a set of sensors operating in two different devices: a wearable suit and a table-top rehabilitation device. On one side the former is intended to provide an estimation of arm posture and muscular stress, while the latter, MOTORE++, performs a series of exercises by exerting and monitoring guidance forces in accordance with the position of the device.

* This work has been funded by European Commission in the ECHORD++ project (FP7-ICT-601116)

¹All authors are with TeCIP Institute of Scuola Superiore Sant'Anna, Italy. Contact n.lastname@sssup.it



Fig. 1. User interacting with the MOTORE++ device: the user sits at the desk holding the device handle where a XY force cell is present. The arm is resting on the arm holder. A counterweight is used to balance the device. During rehabilitation exercises, the user can move the mobile robot all over the desk. In the meanwhile the user wears the wearable 5 DoF system. The armband on the upper arm contains an IMU unit and the EMG add-on, while the other two bands at wrist and torso contain IMU units.

The method is based on sensor fusion to achieve a valid metric for the evaluation of the patient condition with the integrated system. In accordance with common practice in literature [9] we extract three evaluation parameters: Force Directional Error (FDE), Work Efficiency (WE) and Mean Work (meanW). The wearable sensors, instead, return information of joint angles and 8 EMG signals, useful to evaluate muscular activity/weakness(MVC) and the co-activation ratio (CoA), parameter to detect abnormal intra-limb synergies through principal component analysis [7].

The paper is organized as follows: Section II presents the characteristics and the design of the MOTORE++ device. Section III shows how the wearable sensor system has been structured. Section IV describes the choice and the composition of the assessment exercise and Section V illustrates the criteria of construction of our metric. In Section VI we report the experimental results.

II. MOTORE SYSTEM

The mobile haptic-rehabilitation system, MOTORE++, is depicted in Fig. 1. The shape and concept of the system is similar previous MOTORE device [1], but electronics and control logic is completely new [20].

MOTORE is a portable, mobile haptic interface using its wheels to deploy rehabilitation exercises. The haptic interface is equipped with a load cell in the handle as force sensor and allows interaction between the user and the

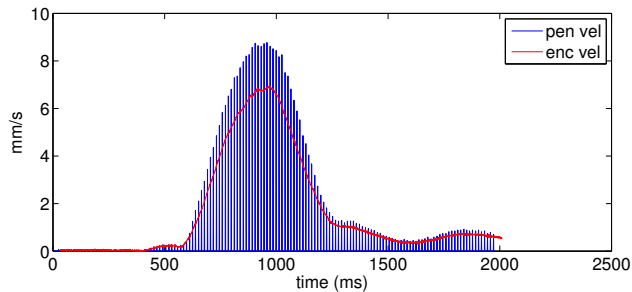


Fig. 2. Measures of encoder velocity and pen velocity in mm/s aligned using estimated delay via cross correlation when an external impulse is given to the device.

robot omni-directional wheels to generate force feedback. The analysis of the kinematics is available in [3] and [8]. MOTORE++ is a technology shift enhancement improvement over the previous version and demonstrates greater versatility in combination with high stability and robustness. The weight of the robot is 10.5 Kg and the new location of center of mass allows to exert higher forces thanks to the counterweight. In terms of electronics, MOTORE++ employs the new ARM Cortex M7 processor family that allows very high on-board computation capabilities (1082 CoreMark / 462 DMIPS) and internal hardware support to double precision floating point operations. Lithium Batteries allow to run the system autonomously for almost one hour, and in addition an easy battery replacement slot allows to swap batteries without interrupting rehabilitation session. Such characteristic is considered high useful in clinical setups where rehabilitation session are delivered regularly each 15 and 30 minutes.

One of the most relevant innovations of this version of the device is a novel sensor fusion policy that exploit an optimized haptic rendering and a precise localization system, realized with Anoto technology¹. MOTORE++ integrates an optical sensor that reads a known pattern printed on the desk to localize accurately the position and orientation of the device, and combines this information with internal data coming from moving wheels. As a consequence MOTORE++ absolves tracking tasks with minimal error and provides a good choice in terms of control constructions and trajectory design. At the base of the fusion there is the measurement of the pen 2D linear (with 0.03mm resolution) and angular rotation. The information from the pen and from the encoders readings is properly used in an Extended Kalman filter (EKF) filter running at 1kHz for estimating the absolute position of the device over the desk. In previous work the pen was connected via Bluetooth while in MOTORE++ it is embedded with a stable rate of 75Hz and measured delay of 30ms as shown in Figure 2. The delay is taken into account in the filter via history update and fast forward prediction.

The loading cell has been calibrated using manufacturer information and the residual offset is removed at startup doing a statistical force analysis when the handle is ungrasped.

¹<http://www.anoto.com>

A. Control structure and specific implementation

MOTORE++ has a multithreaded control systems that runs several loops in parallel. Two major control loops in the device do provide the generation of the force feedback: an internal current controller running at 5KHz and a force-position controller running at 1KHz. The internal DMA samples motor currents at 40KHz, then the current controller averages these samples and uses the estimated value to regulate the appropriate PWM duty cycle to the h-bridges. The controller structure also includes a feed-forward component that compensates for the expected current using the ideal switching model, and a feedback controller (a PI regulator) that uses the sensors' values to cancel the current error.

The force-position control loop developed for the execution of the exercise is governed by the following equations:

$$Fp = (\alpha \cdot k \cdot (Pd - P) + (1 - \alpha) \cdot Fh)^T \cdot vp \cdot vp \quad (1)$$

$$Fo = (k \cdot (Pd - P))^T \cdot vo \cdot vo \quad (2)$$

$$Ft = Fp + Fo \quad (3)$$

$$Ft = Ma \cdot a + b \cdot v \quad (4)$$

Where,

- Pd is the desired position as derived from the constrained motion policy/exercise;
- P is the actual position;
- k is the desired stiffness to gently attract the user towards the motion trajectory;
- $\alpha \in [0, 1]$ is a tunable parameter to switch between an admittance/impedance controller;
- vp is the versor parallel to the desired motion trajectory (computed in Pd);
- vo is the versor orthogonal to the desired motion trajectory (computed in Pd);
- Ma is the apparent mass to reflect in admittance operation,
- b is the apparent viscosity parameter,
- a is the estimated acceleration.

Below the specific function absolved for the control in each equation.

Admittance (1): the first equation computes commanded force in the direction of motion parallel the exercise trajectory. The equation introduces a switch (α) to variate the style of motion. When $\alpha = 1$, a completely passive motion is considered and the robot moves to the desired position by ignoring the force exerted on the handle; when $\alpha = 0$, the motion is completely guided by user force exerted along the exercise direction on the device.

Impedance (2): the second equation computes the rendering force profile in the direction of motion orthogonal the exercise trajectory. In this case we implement a pure impedance force that is proportional to the distance between the actual device position and the trajectory.

Total commanded force (3): the overall force is the combination of admittance and impedance force.

Velocity command (4): internally MOTORE uses a unique

velocity controller obtained from the integration of estimated acceleration information. Hence in eq. (4) we combine viscous effects and the Ft to estimate the velocity at device handle.

The logic of MOTORE++ is managed using additional loops: a control monitor (1KHz) implements diagnostics and basic behaviors of the robot, and a higher level control (100Hz) manages external communication with a remote virtual environment and allows to accept/reject external commands for the execution of rehabilitation tasks. The force position controller is also composed of the aforementioned EKF to reconstruct the robot location at 1KHz, thus providing a constant position estimation for the internal velocity/position controller (internal loop).

III. WEARABLE SYSTEM INTEGRATION

The wearable suit has been originally designed for the purpose of assessment of musculoskeletal disorders during daily work activity [16] with upper limb motion tracking [15] combined with wearable electromyographic measurements.

The motion reconstruction is achieved with the implementation of a kinematic model based on Denavit-Hartenberg method at 5 or 7 Degree of Freedoms (DoFs), depending if the tracking of wrist movements is required or not. In the 7 DoF configuration 7 joint-angles are registered: (i) shoulder abduction/adduction angle, flexion/extension angle, prono-supination angle; (ii) elbow flexion/extension angle, prono-supination angle; (iii) wrist flexion angle and abduction/adduction angle. The wearable device is composed of 3 or 4 IMUs respectively for the 5 and 7 DoFs model, each equipped with tri-axial gyroscope, accelerometer and magnetometer (Invensense 9250). Due to the non linearity of the kinematic model, an Unscented Kalman Filter (UKF) has been employed. The device exploits a system for the capture of surface EMG signals to assess arm muscular activity and the possible abnormalities. Surface button electrodes have been connected to each of 8 channels for EMG registration and 2 channels have been used for the reference EMG and RLD.

IV. ASSESSMENT EXERCISE

To reach our analysis aims, we've chosen a Point-to-Point reaching exercise (PtP) in Free/Constrained Target mode. The exercise has been structured in 4 tasks: horizontal, vertical and two diagonal directions movements. Each task is composed of 2 passive and 2 active trials. To assist the user in the active phase of motion an help modality has been added: in the case the user is keeping staying in the same point of the trajectory for more than 10 seconds, the robot enters in a passive modality for a short stretch of the trajectory. The three sensor units for the arm motion reconstruction are placed respectively on forearm, arm and chest. The EMG electrodes are positioned in pairs on the epidermic area corresponding to the Pectoralis Major(PM),Biceps Brachii(BB),Middle Deltoid(MD) and Triceps Brachii(TB) muscles as shown in fig. 3.

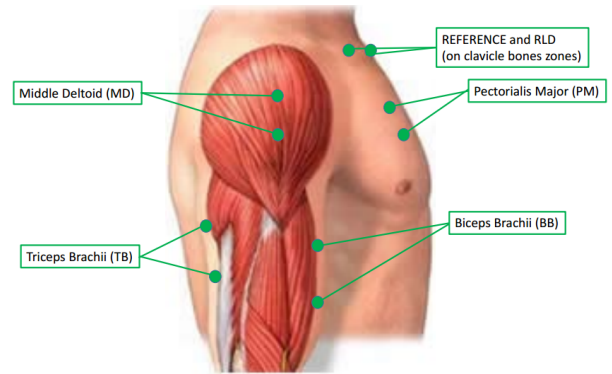


Fig. 3. EMG electrodes positioning: detail of zones of superficial application of EMG buttons.

V. DATA ANALYSIS

The intent of this task is to develop a metric of assessment of affected people based on the comparison with healthy persons performance if subject to the same test. We choose to conduct a wide spectrum analysis on upper limb force capability together with muscular synergies and activity. On the human-robot force exchange side we focused our attention on 3 indexes: Mean Work (MW), Work Efficiency(WE) and Force Directional Error(FDE) [9], [5], [10]. On the muscular side EMG inspection of weakness was conducted through Maximum Voluntary Contraction (MVC) analysis and synergies evaluation achieved via Principal Component Analysis (PCA) and Co-Activation Ratio formulation [17], [19]. The details of these metrics are discussed in the following sub-sections.

All data produced by the system is timestamped for synchronization and sent via TCP over Wireless 802.11n to a data fusion and extraction node running on a computer. This node collects wearable sensors's data IMU at 100Hz, and EMG at 500Hz. The data from the MOTORE++ device is acquired at 200Hz including position, velocity, force and device status. Such data is used for pose reconstruction and EMG filtering, then combined with the MOTORE++ information for the computation of the metrics

A. Force Analysis

Data of active and passive subjects' force profiles of planar XY components were extracted by MOTORE++ during the exercise execution².

Force Directional Error. Parameter evaluating direction of forces exerted on the XY directions. It is quantified as the relation between the singular affected subject force vector and the mean force vector registered in healthy people tests (eq. 7). The force vector is obtained as the contribution of voluntary force profile during each phase of motion averaged on the total trials (eq. 6). Voluntary force profile is obtained as the difference between the force profiles registered during

²The device uses a global reference system centered in the geometrical center of the sliding panel (see fig. 1) with axis aligned to the borders, X → left to right, Y → bottom to up.

active phases of motion and the mean of passive test phases (eq. 5).

$$p^j(t) = \frac{1}{trp} \cdot \sum_{i=1}^{trp} p_{i=1}^j(t) \quad (5)$$

$$F^j = \frac{1}{trt} \cdot \sum_{i=1}^{trt} \frac{\sum_{t=t_0}^{t_f} a_i^j(t) - p^j(t)}{N} \quad (6)$$

$$FDE = \arccos \left(\frac{\vec{F}_{subj} \cdot \vec{F}_{healthy}}{|\vec{F}_{subj}| \cdot |\vec{F}_{healthy}|} \right) \quad (7)$$

with t_0 = initial time, t_f = final time, j = index indicating force component considered (x and y in our case), i = index indicating the tasks, trt = sum of passive and active trials, N = samples total number, \vec{F}_{subj} = force vector of tester, $\vec{F}_{healthy}$ = mean value of healthy testers force vector.

Mean Work and Work Efficiency. MW is a parameter obtained averaging through the exercise tasks the value of *positive work* done by the upper arm during the test (eq. 8). WE indicator has values in the range [0,1] ($\eta = 1$ represents the optimal ideal performance) and it has been calculated as the ratio (eq. 10) of *positive work* respect *potential work* (eq. 10).

$$W_i = \sum_{t=t_0}^{t_f} \left\{ \sum_{j=1}^2 \max \left\{ [a_i^j(t) - p^j(t)] \times \Delta_i^j(t), 0 \right\} \right\} \quad (8)$$

$$\Theta_i = \sum_{t=t_0}^{t_f} \left\{ \sqrt{\sum_{j=1}^2 [a_i^j(t) - p^j(t)]^2} \times \sqrt{\sum_{j=1}^2 [\Delta_i^j(t)]^2} \right\} \quad (9)$$

$$\eta_i = \frac{W_i}{\Theta_i} \quad (10)$$

with t_0 = initial time, t_f = final time, j = index indicating force component considered (x and y in our case), i = index indicating the tasks, trp = number of passive trials, Δ_i^j = vector containing the piece of trajectory traveled from the previous to the current sample time.

B. EMG Analysis

EMG signals were extracted by wearable sensors during the exercise execution. Below post-processing of data and laws implemented.

Co-Activation Ratio. Detector of abnormal co-contraction in antagonistic proximal muscles (PM-BB and MD-TB) if positive values are assumed [6] [7]. First the data are filtered with a bandpass filter Butterworth filter (order 8, frequencies range [10-250]Hz) and an adaptive FIR filter based on LMS algorithm and on a noise model formulated ad hoc for our device. Then 4 of the 8 raw EMG signals collected during the exercise are chosen (1 for every muscle bundle of interest) and the PCA [17] [19] computed. First and second Principal components are used to compute our indicators (CoA ratios) having values in [-1,1] and calculated on every motion direction (8)-(9):

$$c_{1i} = (P_{1i}^{PM} + P_{1i}^{BB})(P_{1i}^{MD} + P_{1i}^{TB}) \quad (11)$$

$$c_{2i} = (P_{2i}^{PM} + P_{2i}^{BB})(P_{2i}^{MD} + P_{2i}^{TB}) \quad (12)$$

with c_{1i}, c_{2i} = CoA ratios respect to 1st and 2nd PC for the i-th task (motion direction, P_{1i}^X = correlation coefficient between 1st principal component and EMG of X muscle in the i-th task).

MVC analysis. Root Mean Square algorithm followed by Power Spectral Density analysis were conducted in order to evaluate the percentage of muscular activation of the limb during the test. We detect weakness for each muscle as percentage under the ranges established on the based of normal limb activity registered on healthy subjects. In this case we determine Maximal Voluntary Contraction not as maximal isometric muscular contraction possible for the subject, but in terms of maximal contraction applied by the tester while executing the exercise.

C. Validation of exercise

Joints angles have been collected from wearable sensors. Their temporal evolution along the different tasks suggest a validation protocol of the exercise. If the exercise is well-executed, a particular behavior is expected otherwise the subject has moved the chest and hold the arm at the same position: in *horizontal direction (TASK 1)* the shoulder abduction angle significantly variable and elbow flexion angle almost constant or little changing; while in *vertical direction (TASK 3)* the shoulder and elbow flexion angle significantly variable.

VI. EXPERIMENTAL RESULTS

The validation of the constructed metric has been conducted in the rehabilitation clinic Auxilium Vitae, Volterra. The validation was performed with 18 healthy subjects (8M/10F with average age 30) and 10 affected subjects (4F/6M with age 65 ± 12). Fig.VI summarizes the relevant results. The columns represents: c_{ij} = *theCoA* Ratio of i-th task relative to j-th PC; then the percentage of activation during the exercise for each muscle; Fx,Fy = mean force among all exercises, FDE = force directional error, WE = work efficiency, W = positive work. Expected ranges, from healthy subjects, were reported in the last row and used as comparison parameter for anomaly detection. Abnormal synergies and muscular weakness have been detected in some subjects and are reflected also in the EMG profiles processed with RMS in frequency domain (see fig.4). In most cases, subjects demonstrated a lower level of muscular activation during the execution of the exercise when compared with the expected ranges. As an example, see fig.4, apart of a general altered EMG profile of the stroke subject and the frequent co-activation of antagonistic fibers, we notice that the initial Pectoralis Major muscle contribution is very low. This phenomenon is associated to the low value of weakness parameter registered for PM in the table of results, Subject 1. Other subjects, instead, have shown great weakness (up

Results Table															
Subj	SINERGY								WEAKNESS (% musc.activity)				FORCES		
	c_{11}	c_{12}	c_{21}	c_{22}	c_{31}	c_{32}	c_{41}	c_{42}	PM	BB	MD	TB	FDE	WE	W
1	0.006	0.01	0.002	0.004	-0.001	-0.001	0	0	0.168	0.301	0.237	0.299	180	0.642	5
2	-0.109	-0.112	-0.255	-0.066	-0.038	-0.059	-0.011	-0.016	0.027	0.233	0.145	0.334	180	0.563	17
3	-0.005	0	0	0	0	-0.001	-0.005	-0.008	0.013	0.008	0.017	0.054	122	0.323	7
4	-1.001	0.032	-0.025	-0.007	-0.184	-0.234	-0.008	-0.025	0.13	0.049	0.361	0.262	71	0.543	18
5	-0.001	-0.003	0	-0.001	-0.017	-0.044	-0.012	-0.034	0.157	0.232	0.252	0.146	0	0.6	21
6	-0.144	-0.351	-0.002	-0.003	0.003	0.008	-0.101	-0.319	0.253	0.421	0.22	0.475	0	0.634	29
7	-0.841	-0.034	-0.065	-0.06	-0.164	-0.145	-1.001	0.031	0.473	0.3	0.265	0.297	99	0.627	43
8	0	-0.002	-0.013	-0.02	-0.04	-0.007	-0.077	-0.009	0.102	0.299	0.046	0.256	85	0.584	47
9	-0.14	-0.013	-0.133	-0.014	-0.065	-0.132	-0.126	-0.019	0.231	0.33	0.144	0.156	0	0.572	9
10	-0.003	-0.003	-0.093	-0.001	-0.005	-0.011	-0.024	-0.029	0.018	0.062	0.04	0.221	136	0.341	4
Fit Subj.	VALUES in $[-1, 0]$ Common range: $[-0.6 -0.2]$								Values in $[0, 1]$ Common ranges: $[0.3, 0.45]$				FDE: Low Val. (≥ 0) WE in $[0, 1]$ WE range: $[0.65, 0.8]$ W range: $[8, 30]$		

TABLE I
INDEX OF PERFORMANCE FOR 10 AFFECTED SUBJECTS VERSUS HEALTHY COMMON VALUES.

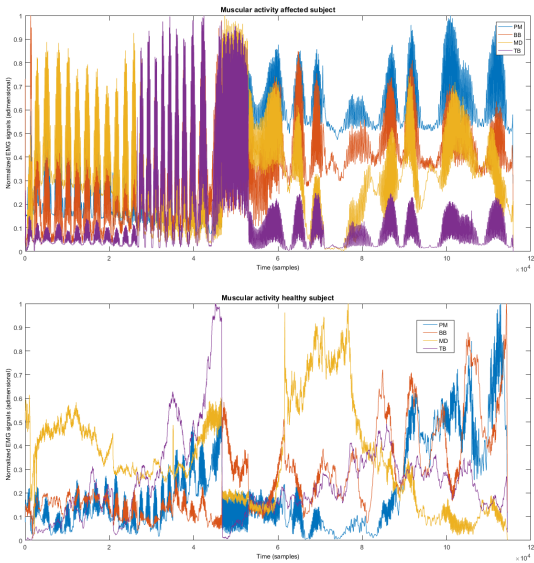


Fig. 4. EMG data for Subject1 (Upper) and one healthy subject (lower). RMS values of PM, BB, MD and TB muscles are showed vs time. RMS values are normalized against their peak values. We note the overlap of activity between the antagonistic pair of muscles (PM-BB and MD-TB) in the affected profile.

to 1% of muscular activation) even in more than a singular muscular fiber but not a synergy relevant anomaly. This is probably due to the variegated sample of illnesses having neurological or mechanical post-traumatic events, and different aging since the trauma.

Underlined disorders in the direction of forces exerted by the ill subjects or a Work Efficiency under the ranges of healthy people correspond to an altered user forces profile over time. For instance, Subject 2 was victim of a spasmodic status during the execution of the test with the consequent alteration in measured force direction (FDE index) and in the efficiency of total work. In many cases it emerges a correlation between force abnormalities (in par-

ticular FDE) and electromyographic evaluation (i.e. Subject 1 in VI). These phenomena depend on the link between force registered and muscular activity: information on force directions and entities can be extracted from EMG signals in terms of contractions of singular muscle fibers and co-contraction between different muscles. The co-contraction of antagonistic muscles can cause undesired deviation of force direction as common in spasmodic events. However, upper limb rehabilitation is applied on illnesses due to different occurred trauma of neurological or mechanical post-traumatic origin and neither all considered factors nor a particular combination coexist coherently in every case. Moreover, the samples of ill people tested differ also in time passed from the traumatic event to the assessment analysis. As a consequence, correct evaluation of illness seems to require both analysis (forces and muscular activity) because there is not a most indicative index, but every specific pathology could present even only one alteration of all that we have considered in our metric.

VII. CONCLUSION

In this work we showed how the integrated information collected from a mobile haptic rehabilitation robot and a wearable system provides insight in the evaluation of motor disabilities. We focused on the aspect of muscular and force measures with the aim of differentiating patients and healthy subjects through different computed measures. A set of seven weakness and force indicators were automatically extracted by the system during the operation. A clear distinction was highlighted by the scored indexes not only between healthy and the affected subjects but also within each specific subject when any sort of spasmodic event occurs. The preliminary results show high confidence to use this metric for extensive patient validation.

Future improvements aim to refine joint arm pose estimation between wearable sensors and localization sensor for the mobile device thus removing related issues on slow yaw-drift of the IMUs due to magnetic interference.

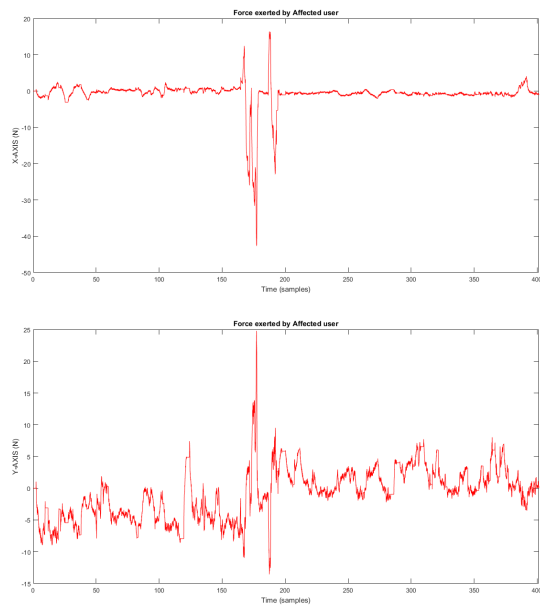


Fig. 5. Affected subject force profile (Subject 2). Module of forces of stroked subject reaches 40 N showing the presence of a spasm. The event is reflected in score values of FDE and WE.

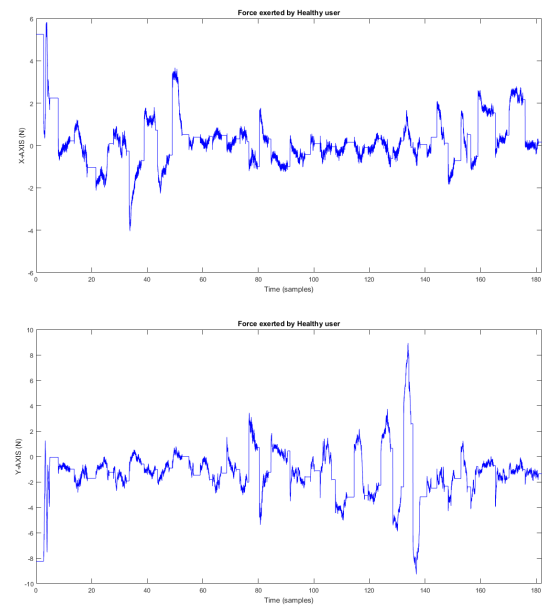


Fig. 6. Healthy subject force profile. Module of forces never exceed 10N.

REFERENCES

- [1] C. Avizzano, M. Satler, G. Cappiello, A. Scoglio, E. Ruffaldi, M. Bergamasco, et al. Motore: A mobile haptic interface for neuro-rehabilitation. In *RO-MAN, 2011 IEEE*, pages 383–388. IEEE, 2011.
- [2] C. Burgar, P. Lum, P. Shor, and M. Van der Loos. Development of robots for rehabilitation therapy : The palo alto va/stanford experience. *J. of Rehabilitation Research and Development*, 37:6:663–673, 2000.
- [3] B. Carter, M. Good, M. Dorohoff, J. Lew, and R. L. W. Li. Mechanical design and modeling of an omni-directional robocup player. In *in Proceedings RoboCup 2001 International Symposium*, 2001.
- [4] D. Chen, A. Song, and A. Li. Design and calibration of a six-axis force/torque sensor with large measurement range used for the space manipulator. In *Procedia Engineering*.
- [5] R. Colombo, I. Sterpi, et al. Measuring changes of movement dynamics during robot-aided neurorehabilitation of stroke patients. *IEEE Trans. on Neural Systems and Rehab Engineering*, 18:1:1534–4320, 2010.
- [6] P.-C. Kung, C.-C. Lin, and M.-S. Ju. Reducing abnormal synergies of forearm, elbow, and shoulder joints in stroke patients with neuro-rehabilitation robot treatment and assessment. *Journal of Medical and Biological Engineering*, 32:2:139–146, 2009.
- [7] P.-C. Kung, C.-C. Lin, and M.-S. Ju. Neuro-rehabilitation robot-assisted assessments of synergy patterns of forearm, elbow and shoulder joints in chronic stroke patients. *Clinical Biomechanics*, 25:647–654, 2010.
- [8] Y. Liu, R. Williams, and J. Zhu. Integrated control and navigation for omni-directional mobile robot based on trajectory linearization. In *American Control Conference, 2007. ACC'07*, pages 2153–2158. IEEE, 2007.
- [9] P. Lum, C. Bugar, D. Kennedy, and H. Van der Loos. Quantification of force abnormalities during passive and active-assisted upper-limb reaching movements in post-stroke hemiparesis. *IEEE Tran on Biomedical Engineering*, 46(6):652–662, 1999.
- [10] P. Lum, C. Bugar, and P. Shor. Evidence for improved muscle activation patterns after retraining of reaching movements with the mime robotic system in subjects with post-stroke hemiparesis. *IEEE Trans. on Neural Systems and Rehab Engineering*, 12:2:1534–4320, 2004.
- [11] P. Maciejasz, J. Eschweil, K. Gerlach-Hann, A. Jansen-Troy, and S. Leonhardt. A survey on robotic devices for upper limb rehabilitation. *J. of NeuroEngineering and Rehabilitation*, 11:3:1–29, 2014.
- [12] C. McGibbon, A. Sexton, M. Jones, and C. O’Connell. Elbow spasticity during passive stretch-reflex: clinical evaluation using a wearable sensor system. *J. of NeuroEngineering and Rehabilitation*, 10:61, 2013.
- [13] A. Mullick, N. Musampa, A. Feldman, and M. Levin. Stretch reflex spatial threshold measure discriminates between spasticity and rigidity. *Clinical Neurophysiology*, 124:740–751, 2013.
- [14] N. Nordin, S. Xie, and B. Wnsche. Assessment of movement quality in robot-assisted upper limb rehabilitation after stroke: a review. *Journal of NeuroEngineering and Rehabilitation*, pages 11–137, 2014.
- [15] L. Peppoloni, A. Filippeschi, E. Ruffaldi, and C. Avizzano. A novel 7 degrees of freedom model for upper limb kinematic reconstruction based on wearable sensors. In *2013 IEEE 11th International Symposium on Intelligent Systems and Informatics (SISY)*, pages 1–11. IEEE, 2013.
- [16] L. Peppoloni, A. Filippeschi, E. Ruffaldi, and C. Avizzano. A novel wearable system for the online assessment of risk for biomechanical load in repetitive efforts. *International J. of Industrial Ergonomics*, 52:1–11, 2016.
- [17] M. Perez and M. Nussbaum. Principal components analysis as an evaluation and classification tool for lower torso semg data. *J. of Biomechanics*, 36:1225–1229, 2003.
- [18] B. Rohrer, S. Fasoli, H. I. Krebs, R. Hughes, B. Volpe, W. Frontera, j. Stein, and N. Hogan. Movement smoothness changes during stroke recovery. *The Journal of Neuroscience*, 22:18:8297–8304, 2002.
- [19] H. Sadeghi, F. Prince, S. Sadeghi, and H. Labelle. Principal component analysis of the power developed in the flexion/extension muscles of the hip in able-bodied gait. *Medical Engineering & Physics*, 22:703–710, 2000.
- [20] L. Saracino, C. A. Avizzano, E. Ruffaldi, G. Cappiello, Z. Curto, and A. Scoglio. Motore++ a portable haptic device for domestic rehabilitation. In *Proc. of the 42nd IEEE Annual Conference of Industrial Electronics Society (IECON)*, 2016.
- [21] F. Tamar and H. Neville. The coordination of arm movements: An experimentally confirmed mathematical model. *The Journal of Neuroscience*, 5:7:1688–1703, 1985.
- [22] A. A. Timmermans, H. A. Seelen, R. D. Willmann, and H. Kingma. Technology-assisted training of arm-hand skills in stroke: concepts on reacquisition of motor control and therapist guidelines for rehabilitation technology design. *J. of NeuroEngineering and Rehabilitation*, 6:1:1–29, 2009.
- [23] L. Zollo, L. Rossini, M. Bravi, G. Magrone, S. Sterzi, and E. Guglielmelli. Quantitative evaluation of upper-limb motor control in robot-aided rehabilitation. *Med Biol Eng Comput*, 49:1131–1144, 2011.